Higher-Order Human Telomeric G-Quadruplex DNA Metalloenzymes Enhance Enantioselectivity in the Diels-Alder Reaction

ARTICLE *in* CHEMBIOCHEM · FEBRUARY 2015

Impact Factor: 3.09 · DOI: 10.1002/cbic.201402692 · Source: PubMed

5 AUTHORS, INCLUDING:

Yinghao Li
Dalian Institute of Chemical Physics
10 PUBLICATIONS **120** CITATIONS
SEE PROFILE

Mingpan Cheng
Dalian Institute of Chemical Physics
4 PUBLICATIONS **4** CITATIONS
SEE PROFILE

Can Li
Guiyang university
502 PUBLICATIONS **14,880** CITATIONS
SEE PROFILE

ChemPubSoc Europe

DOI: 10.1002/cbic.201402692

CHEMBIOCHEM Full Papers

Higher-Order Human Telomeric G-Quadruplex DNA Metalloenzymes Enhance Enantioselectivity in the Diels–Alder Reaction

Yinghao Li,[a, b] Guoqing Jia,[a] Changhao Wang,[a, b] Mingpan Cheng,[a, b] and Can Li*[a]

Short human telomeric (HT) DNA sequences form single G-quadruplex (G_4) units and exhibit structure-based stereocontrol for a series of reactions. However, for more biologically relevant higher-order HT G_4-DNAs (beyond a single G_4 unit), the catalytic performances are unknown. Here, we found that higher-order HT G_4-DNA copper metalloenzymes (two or three G_4 units) afford remarkably higher enantioselectivity (>90% *ee*) and a five- to sixfold rate increase, compared to a single G_4 unit, for the Diels–Alder reaction. Electron paramagnetic resonance (EPR) and enzymatic kinetic studies revealed that the distinct catalytic function between single and higher-order G_4-DNA copper metalloenzymes can be attributed to different Cu^{II} coordination environments and substrate specificity. Our finding suggests that, like protein enzymes and ribozymes, higher-order structural organization is crucial for G_4-DNA-based catalysis.

Introduction

Nucleic acid structure-related enantioselective catalysis has become a fascinating field of research.[1] RNA can fold into active three-dimensional structures to facilitate reactions with high enantioselectivity.[2] In past decades, DNA structure-based stereochemical control of chemical reactions has been an active area of research.[3] Roelfes and Feringa constructed a series of double-stranded (ds) DNA metalloenzymes and demonstrated the excellent enantioselectivity of dsDNA in a variety of reactions.[4] When the chirality of dsDNA is changed by using unnatural L-DNA, the opposite enantioselectivity was obtained in these reactions.[5] Besides the canonical DNA double helix, other noncanonical DNA structures have also been found.[6] For example, human telomeric (HT) DNA contains a single-stranded 3′-overhang with a d(TTAGGG) repeat that can intramolecularly form a four-stranded DNA structure, called G-quadruplex DNA (G_4-DNA).[7] By virtue of the underlying structural polymorphism[8] together with its possible chiral diversity,[9] HT G_4-DNA is attracting increasing interest for enantioselective catalysis. Moses and co-workers first introduced HT G_4-DNA as a chiral scaffold for enantioselective catalysis: Cu^{II}–bipyridine complexes were used as cofactors to construct HT G_4-DNA metalloenzymes.[10a] Subsequently, a similar strategy was reported by Hennecke's group with Cu^{II}–porphyrin as the cofactor.[10b] Previously, we developed another type of HT G_4-DNA metalloenzyme by directly coordinating a metal ion cofactor (Cu^{II}) to HT G_4-DNAs.[10c–e] Although the cofactors within HT G_4-DNA metalloenzymes are different, these studies clearly indicated that the enantiomeric outcome is strongly dependent on the HT G_4-DNA conformation. However, all HT G_4-DNA metalloenzymes reported so far employed a single G_4 unit (less than 30 bases).

In fact, the single-stranded HT DNA 3′-overhang in cells is 100–200 nt long, and can fold into higher-order HT G_4-DNA with multiple consecutive G_4 units.[11] In a study of catalytic performance of a G_4-DNA–hemin system, it was shown that higher-order G_4-DNA displays enhanced peroxidase-mimicking ability compared with a single G_4 unit.[12] In addition, higher-order G_4-DNA (a target for anticancer drug design) shows a binding behavior for drugs different to that of a single G_4 unit.[13] Importantly, the groups of Qu[13b] and Sugiyama[14] showed that higher-order HT G_4-DNAs display distinct chiral discrimination for chiral drugs. This inspired us to focus on the structure and function of higher-order HT G_4-DNAs in enantioselective catalysis.

Here, higher-order HT G_4-DNA metalloenzymes were constructed, and their catalytic performances were studied (Figure 1). For the Diels–Alder reaction catalyzed by HT G_4-DNA copper metalloenzymes, we found that there is a substantial difference in catalytic performance between a single G_4 unit and higher-order HT G_4-DNAs (two or three G_4 units). In particular, in the presence of 150 mM K^+ (intracellular concentration), higher-order HT G_4-DNA metalloenzymes showed a reaction rate five- to sixfold higher than for a single G_4 unit. More importantly, the enantioselectivity of the reaction was markedly enhanced: from 14% *ee* for a single G_4 to over 90% *ee* for higher-order HT G_4-DNAs. Electron paramagnetic resonance (EPR) spectroscopic studies and Michaelis–Menten kinetics

[a] *Y. Li,[+] Dr. G. Jia,[+] Dr. C. Wang, M. Cheng, Prof. Dr. C. Li*
State Key Laboratory of Catalysis
Dalian Institute of Chemical Physics, Chinese Academy of Sciences
457 Zhongshan Road, Dalian, 116023 (China)
E-mail: canli@dicp.ac.cn

[b] *Y. Li,[+] Dr. C. Wang, M. Cheng*
University of Chinese Academy of Sciences
No.19A Yuquan Road, Beijing, 100049 (China)

[+] *These authors contributed equally to this work.*

Supporting information for this article is available on the WWW under http://dx.doi.org/10.1002/cbic.201402692.

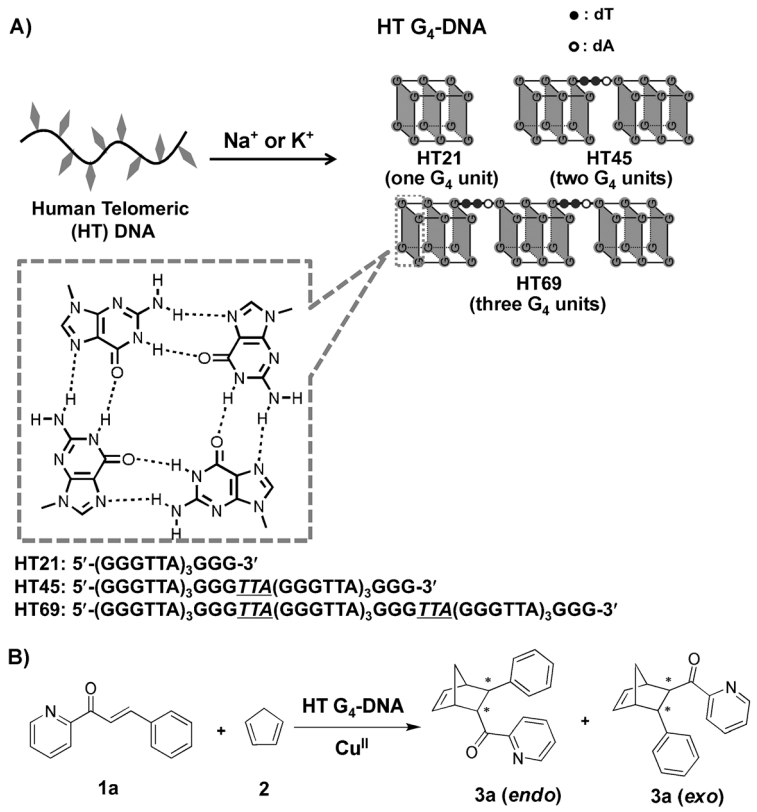

Figure 1. A) HT G_4-DNAs. HT21 represents HT G_4-DNA (single G_4 monomer). HT45 and HT69 represent higher-order HT G_4-DNAs (two or three G_4 units, respectively). Na^+ or K^+ was used to stabilize and adjust the conformation of the G_4-DNAs. TTA = linker residues. B) Model Diels–Alder reaction catalyzed by HT G_4-DNA copper metalloenzymes, assembled by HT G_4-DNAs and $Cu(NO_3)_2$. * = stereocenter.

demonstrated that the higher-order HT G_4-DNAs provide a single Cu^{II} coordination environment and possess excellent substrate specificity, thus making them function as a high-performance metalloenzyme in efficient enantioselective catalysis.

Results and Discussion

Comparison of catalytic performance of HT G_4-DNA metalloenzymes between a single G_4 unit and higher-order HT G_4-DNA metalloenzymes with two or three G_4 units

Table 1 shows the results of the model Diels–Alder reaction catalyzed by monomeric (HT21), dimeric (HT45), and trimeric (HT69) HT G_4-DNA copper metalloenzymes. In the case of Na^+, monomeric HT21-Na-Cu yielded 50% *ee* of the major *endo* diastereomer (Table 1, entry 2). Upon increasing the G_4 units to two (HT45) and three (HT69), the enantioselectivities decreased to nearly zero (Table 1, entries 3 and 4). At the same time, the catalytic activities of HT45-Na-Cu (k_{rel} = 1.2) and HT69-Na-Cu (k_{rel} = 1.0) reduced relative to that of HT21-Na-Cu (k_{rel} = 3.0; Table 1, entry 2 vs. 3 and 4).

In the presence of K^+ (Table 1, entries 5–7), a sharp contrast in enantioselectivity between monomer (HT21-K-Cu) and multimers (HT45-K-Cu and HT69-K-Cu) was observed, but the trend was completely opposite to that for Na^+. The enantioselectivity of the major *endo* diastereomer was low (14% *ee*) for HT21-K-Cu (Table 1, entry 5), but was over 90% *ee* for dimeric HT45-K-Cu and trimeric HT69-K-Cu (Table 1, entries 6 and 7). Besides the excellent enantioselectivity, the multimeric HT G_4-DNA metalloenzymes in K^+ solution also showed much higher activity than the monomer with single G_4 unit (Table 1, entries 5–7). Compared with Cu^{II} alone as the catalyst, HT45-K-Cu and HT69-K-Cu increased the apparent second-order rate constant (k_{app}) by about 25-fold and 23-fold, respectively (Table 1, entry 1 vs. 6 and 7), whereas HT21-K-Cu provided only a fourfold rate increase (Table 1, entry 5).

When Cu^{II} alone was the catalyst, the major *endo* product was racemic (Table 1, entry 1). Unambiguously, the observed enantioselectivity originated from the chirality of the HT G_4-DNAs (Table 1, entries 2–7). Moreover, the distinct induction of enantioselectivity by the monomer (HT21) and multimers (HT45 and HT69) indicate that the geometry of the catalytic cavity within them is substantially different.

Comparison of the structures of HT G_4-DNA metalloenzymes between a single G_4 unit and higher-order HT G_4-DNA metalloenzymes

The structures of the HT G_4-DNAs were characterized by CD spectroscopy (Figure 2). In the case of Na^+, HT21-Na-Cu, HT45-Na-Cu, and HT69-Na-Cu showed similar spectra, corresponding to an antiparallel conformation (Figure 2 A).[8a,d] This can be explained by the "beads-on-a-string" model proposed by Sugimoto and coworkers, where long telomeric DNA intramolecularly fold into multiple G_4-DNA units with the same antiparallel conformation linked by a TTA linker.[11b] Accordingly, it was expected that HT45-Na-Cu and HT69-Na-Cu would give similar catalytic per-

Table 1. The model Diels–Alder reaction catalyzed by HT G_4-DNA copper metalloenzymes.[a]

	Catalyst	Conv. [%][b]	*endo/exo*[c]	*ee* [%, *endo*][c,d]	k_{rel}[e]
1	No DNA	59	92/8	0	1.0
2[f]	HT21-Na-Cu	96	96/4	50	3.0
3[f]	HT45-Na-Cu	69	92/8	<3	1.2
4[f]	HT69-Na-Cu	60	92/8	<−3	1.0
5[g]	HT21-K-Cu	82	94/6	14	4.0
6[g]	HT45-K-Cu	98	96/4	92	25
7[g]	HT69-K-Cu	98	96/4	90	23

[a] Reaction conditions: **1a** (1 mM, 1 equiv), **2** (15 μL, 100 equiv), G-quadruplex unit (0.05 equiv), $Cu(NO_3)_2$ (0.01 equiv), MOPS buffer (1 mL, 20 mM, pH 6.5), 4 °C, 12 h. [b] Determined for the crude product by HPLC analysis on a chiral stationary phase (Scheme S1); reproducibility ±5%. [c] Determined by chiral-phase HPLC; reproducibility ±5%. [d] Enantiomeric excesses are given only for the *endo* diastereomers of corresponding D-A products. [e] Relative apparent rate constant (Scheme S2 and Table S1). [f] 50 mM NaCl. [g] 150 mM KCl.

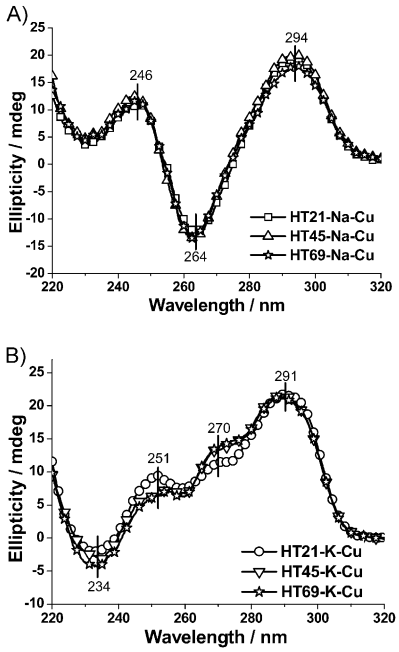

Figure 2. CD spectra of HT G_4-DNA copper metalloenzymes in the presence of A) 50 mM NaCl, or B) 150 mM KCl. CD samples of all HT G_4-DNAs were prepared at 5 μM (G_4 units) in MOPS buffer (20 mM, pH 6.5).

Table 2. The effects of modification of dimeric HT G_4-DNA copper metalloenzymes on the catalytic performance in the model Diels–Alder reaction.[a]

	Sequence (5′→3′)	Conv. [%][b]	*endo*/*exo*[c]	*ee* [%, *endo*][c,d]
The effects of linker residues and linker size				
1	**HT45:** $G_3(TTAG_3)_3\mathbf{TTA}G_3(TTAG_3)_3$	98	96/4	92
2	**HT45-ATA:** $G_3(TTAG_3)_3\mathbf{ATA}G_3(TTAG_3)_3$	>99	96/4	79
3	**HT45-TTT:** $G_3(TTAG_3)_3\mathbf{TTT}G_3(TTAG_3)_3$	>99	96/4	80
4	**HT45-AAA:** $G_3(TTAG_3)_3\mathbf{AAA}G_3(TTAG_3)_3$	93	95/5	72
5	**HT48:** $G_3(TTAG_3)_3(\mathbf{TTA})_2G_3(TTAG_3)_3$	>99	96/4	83
6	**HT51:** $G_3(TTAG_3)_3(\mathbf{TTA})_3G_3(TTAG_3)_3$	98	96/4	82
7	**HT57:** $G_3(TTAG_3)_3(\mathbf{TTA})_5G_3(TTAG_3)_3$	95	96/4	74
8	$(TTA)_{15}$	61	90/10	0
The effects of flanking residues				
9	**HT21-T:** $G_3(TTAG_3)_3\mathbf{T}$	77	91/9	18
10	**HT21-TT:** $G_3(TTAG_3)_3\mathbf{TT}$	90	94/6	48
11	**HT21-TTA:** $G_3(TTAG_3)_3\mathbf{TTA}$	>99	97/3	−37
12	**A-HT21:** $\mathbf{A}G_3(TTAG_3)_3$	64	92/8	−5
13	**TA-HT21:** $\mathbf{TA}G_3(TTAG_3)_3$	95	96/4	78
14	**TTA-HT21:** $\mathbf{TTA}G_3(TTAG_3)_3$	97	96/4	56

[a] Reaction conditions: **1a** (1 mM, 1 equiv), **2** (15 μL, 100 equiv), G-quadruplex unit (0.05 equiv), $Cu(NO_3)_2$ (0.01 equiv), KCl (150 mM), MOPS buffer (1 mL, 20 mM, pH 6.5), 4 °C, 12 h. [b] Determined for the crude product by HPLC analysis on a chiral stationary phase (Scheme S1); reproducibility ±5%. [c] Determined by chiral-phase HPLC; reproducibility ±5%. [d] Enantiomeric excesses are given only for the *endo* diastereomers of the corresponding D-A products.

formances to that of HT21-Na-Cu, provided that active site is within a single G_4 unit. However, this is obviously inconsistent with the fact that there was a significant difference between the monomer (HT21-Na-Cu) and the multimers (HT45-Na-Cu and HT69-Na-Cu; Table 1, entries 2–4). Therefore, it was deduced that the TTA linker region between two adjacent G_4 units of higher-order HT G_4-DNAs might have a great effect on the catalytic performance of higher-order HT G_4-DNA (HT45 and HT69) metalloenzymes.

The CD spectra of HT21-K-Cu, HT45-K-Cu, and HT69-K-Cu show the feature of a hybrid G_4 structure (Figure 2B).[15] Although the accurate structure of multimers in K^+ conditions is still controversial,[11b–d,16] many studies have reached a consensus that two adjacent G_4 units are not fully independent and that quadruplex–quadruplex interaction occurs in the TTA linker region.[16] Therefore, it could be deduced that the enhanced catalytic performance of the multimers might also be related to this exclusive TTA linker region.

Insight into the relationship between the TTA linker and catalytic performance

In view of the excellent catalytic performance and the biological significance of K^+ in the cellular environment,[17] we next focused on the dimeric HT45-K-Cu to get a deeper insight into the relationship between the TTA linker and catalytic behavior. We modified the TTA linker region in two ways: 1) mutation of linker residues, and 2) lengthening the linker. These two modifications would result in a change in the quadruplex–quadruplex interaction.[14,16b–c] When we mutated the linker from TTA to ATA, TTT, or AAA, the enantioselectivity showed a decrease from 92% *ee* to 79, 80, and 72%, respectively (Table 2, entries 1–4). This indicates that TTA might be a conserved sequence for excellent chiral induction.

Dimeric G_4-DNAs with two, three, or five TTA linkers were also tested, as a longer linker can weaken the quadruplex–quadruplex interaction.[14] As listed in Table 2 (entry 1 vs. entries 5–7), with increasing linker length (from one to five TTA repeats), the enantioselectivity showed a gradual decrease, from 92% *ee* to 83, 82, and 74%. The dimeric G_4-DNA (HT57) with a linker of five TTA repeats was thought to be divided into two separate G_4 units, but 74% *ee* was still observed; this is much higher than for monomeric HT21-K-Cu (14% *ee*; Table 2, entry 7 vs. Table 1, entry 5). Furthermore, $(TTA)_{15}$-Cu, which has the same base component as the linker but no G_4 structure, led to an essentially racemic product **3a** (Table 2, entry 8). Considering all these data, it can be postulated that certain bases near one of the G_4 units might cap the end of G_4 and then form a unique structure that enhances chiral induction.[15c,18]

To verify this, we introduced A or T bases into the 3′- or 5′-end of the HT21 sequence to mimic this part of dimeric HT45-K (Table 2, entries 9–14). The 5′- or 3′-flanking residue can change enantioselectivity to a great degree, as compared with HT21-K-Cu. However, the enantioselectivity was much less than the 92% *ee* of dimeric HT45-K-Cu (Table 2, entry 1). In particular, HT21-TTA with flanking TTA residues at the 3′-end resulted in the opposite enantiomer of the *endo* product (Table 2, entry 11). These data strongly suggest that the flanking residues can cap the terminal face of the G_4 unit and form a special

structure. However, it was not able to form a favorable chiral space as for HT45-K-Cu, in order to produce excellent chiral induction. In other words, the unique domain constructed from two adjacent G_4 units and the three-nucleotide TTA linker is necessary for HT45-K-Cu to afford suitable catalytic cavity and excellent enantioselectivity.

Substrate scope

We then tested the enantioselective Diels–Alder reaction of cyclopentadiene (**2**) with other substituted aza-chalcones (**1b**, **1c**; Figure 3). For a substrate with a more hydrophobic group

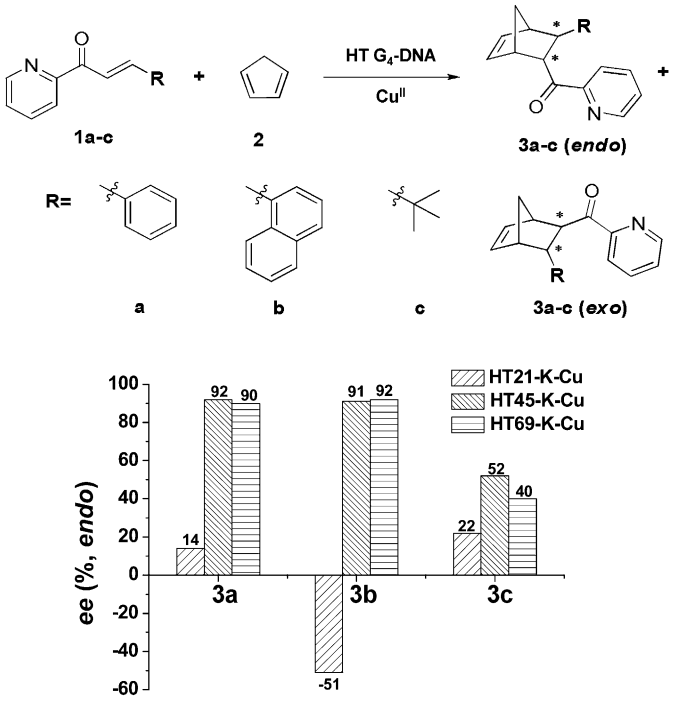

Figure 3. Substrate specificity of HT G_4-DNA copper metalloenzymes for the Diels–Alder reaction (for detailed information see Table S2).

(**1b**: R = α-naphthyl), higher conversion and excellent enantioselectivity (>90% *ee*) were still obtained when catalyzed by HT45-K-Cu and HT69-K-Cu, as compared with HT21-K-Cu (Table S2 in the Supporting Information). This might be partly ascribed to the more hydrophobic TTA linker region in the higher-order HT G_4-DNAs.[12–14] When using **1c** (R = *t*Bu) as the substrate, HT45-K-Cu and HT69-K-Cu also achieved superior enantioselectivity than that of HT21-K-Cu. The similar chiral induction of HT45-K-Cu and HT69-K-Cu indicates that they share a similar chiral cavity for promoting stereochemical control in the reaction. This gives a further support that catalytic sites are most likely located at the unique domain of the higher-order HT G_4-DNA that is constructed from two adjacent G_4 units and a TTA linker. We explored other types of substrates **4a–d** (α,β-unsaturated acylimidazoles) as dienophiles in Diels–Alder reactions, and found that higher-order HT G_4-DNA metalloenzyme still possessed higher catalytic activity and enantioselectivity than for a single G_4 unit (Table S3).

Nature of the active sites: EPR evidence and enzymatic dynamics

In HT G_4-DNA copper metalloenzymes, Cu^{II} serves as the active center for catalyzing the Diels–Alder reaction, and HT G_4-DNA functions as a chiral scaffold for stereochemical control.

Given the properties of a paramagnetic Cu^{II} ion (electronic configuration $3d^9$, $S = {}^1/_2$), we employed continuous-wave (cw) X-band EPR spectroscopy to investigate the coordination environments of the Cu^{II} ion in artificial HT G_4-DNA copper metal-

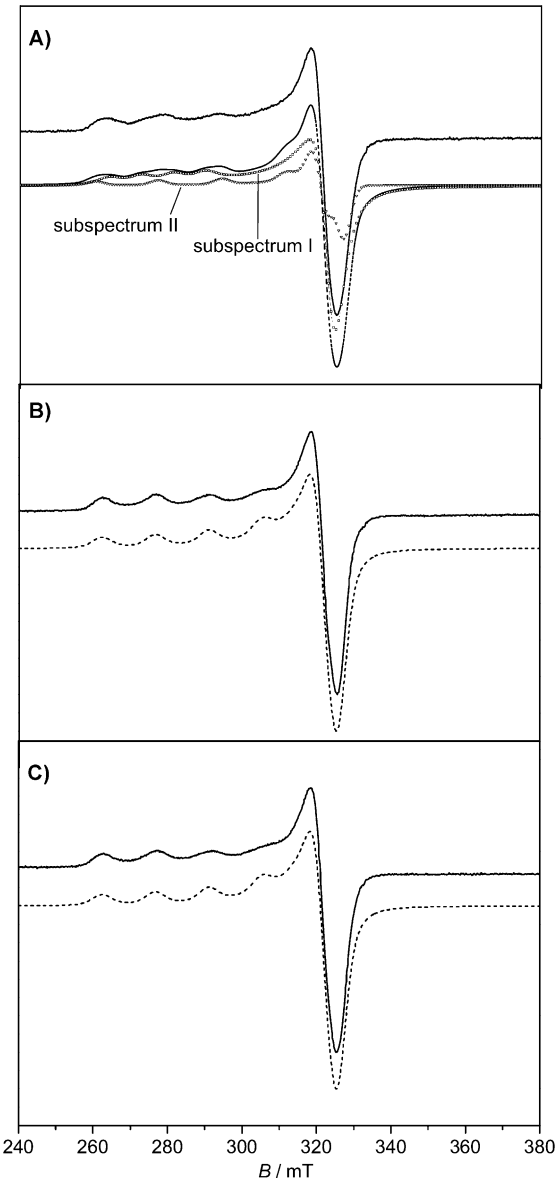

Figure 4. X-band continuous-wave (cw) EPR spectra of HT G_4-DNA copper metalloenzymes: A) HT21-K-Cu (two simulated subspectra are shown), B) HT45-K-Cu, and C) HT69-K-Cu, recorded at 100 K. Experimental conditions: microwave frequency 9.3 GHz, power 5.0 mW, modulation amplitude 6G, modulation frequency 100 KHz. Solid lines: experimental spectra, short dashed lines: simulation spectra.

Table 3. *g* values and Cu^{II} magnetic hyperfine parameters (*A*) of HT G_4-DNA copper metalloenzymes.

Sample		$g_{\parallel}$	$g_{\perp}$	$A_{\parallel}$ [MHz]	$A_{\perp}$ [MHz]	Population [%]
HT21-K-Cu	I	2.407	2.065	285	3	83
	II	2.333	2.075	545	–[a]	17
HT45-K-Cu		2.349	2.072	466	13	100
HT69-K-Cu		2.348	2.071	460	7	100

[a] Not determined.

loenzymes.[19] The EPR spectra of HT21-K-Cu, HT45-K-Cu, and HT69-K-Cu together with their simulations are shown in Figure 4 (simulation parameters in Table 3). The EPR spectrum of HT21-K-Cu was simulated with two subspectra (I and II, Figure 4A). Subspectrum I has a higher-field $g_{\parallel}$ value (2.407) with 83% population, and subspectrum II has a lower-field $g_{\parallel}$ value (2.333) with 17% population. This indicates that there are two types of Cu^{II} coordination environments in HT21-K-Cu. In contrast, the EPR spectra of HT45-K-Cu and HT69-K-Cu could be well simulated by a single spectrum, thus indicating a single Cu^{II} coordination environment (Figure 4B and C). Moreover, the anisotropic *g* values and magnetic hyperfine coupling tensors (*A*) of HT45-K-Cu and HT69-K-Cu displayed nearly the same values (Table 3), which suggests that the Cu^{II} environments are similar. This sharp contrast of Cu^{II} coordination environments between HT45-K-Cu/HT69-K-Cu and HT21-K-Cu is in good agreement with the CD and catalytic results, where HT45-K-Cu and HT69-K-Cu showed similar CD features and comparable catalytic activities but were distinct from those for HT21-K-Cu (Figure 2B and entries 5–7 in Table 1).

Furthermore, a comparison of the Michaelis–Menten kinetics between HT21-K-Cu and HT45-K-Cu shows that the enhancement in catalytic efficiency (k_{cat}/K_M) of HT45-K-Cu is attributable to the decrease in K_M rather than an improvement in k_{cat} (Table 4 and Figure 5). This indicates that the active site within

Table 4. The catalytic activity of HT G_4-DNA metalloenzymes at pH 6.5 in the presence of 12.5 μM Cu^{II}.

Catalyst	k_{cat}/K_M [$M^{-1}s^{-1}$]	$k_{cat}\times10^{-3}$ [s^{-1}]	K_M [μM]
HT21-K-Cu	16 ± 4	6.03 ± 0.60	359 ± 42
HT45-K-Cu	64 ± 5	2.09 ± 0.04	32.6 ± 1.7

HT45-K-Cu is more substrate specific. Therefore, we conclude that the higher-order HT G_4-DNAs (HT45-K and HT69-K) can provide a relatively specific binding site for Cu^{II}, and the resulting active site displays substantial improvements in substrate specificity, which is efficient for enhancing chiral induction as well as catalytic activity in the Diels–Alder reaction.

Conclusion

The relationship between the structure and function of higher-order HT G_4-DNAs has received great attention recently. We focused here on the chiral features of higher-order HT G_4-DNAs and investigated their stereochemical control function. Interestingly, with a biologically relevant concentration of K^+ (150 mM), higher-order HT G_4-DNA copper metalloenzymes can afford remarkably higher enantioselectivity (>90% *ee*) than single G_4-DNA copper metalloenzyme for the model Diels–Alder reaction, as well as a five- to sixfold rate increase. Our results indicate that the specific domain constructed from two adjacent G_4 units and a TTA linker is a critical for the enantioselectivity of higher-order HT G_4-DNA copper metalloenzymes. The EPR spectroscopic results reveal that this specific domain can provide a single Cu^{II} coordination. Enzymatic dynamics further indicate that the resulting active site shows good substrate specificity and efficiently promotes catalytic activity and chiral induction in the Diels–Alder reaction. Our finding suggests that, like protein enzymes and ribozymes, the higher-order structural organization is also crucial for G_4-DNA-based catalysis.

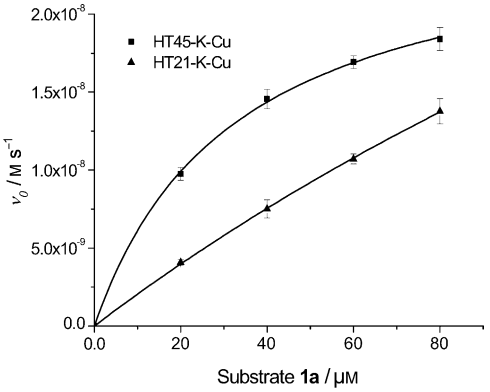

Figure 5. Catalytic activity of HT G_4-DNA metalloenzymes at pH 6.5 in the presence of 12.5 μM Cu^{II}. Smooth curve shows the fit to the Michaelis–Menten equation.

Experimental Section

All DNA oligodeoxynucleotides were purchased from Sangon (Shanghai, China), and the precise DNA strand concentrations were determined by measuring the UV absorbance of sample at 260 nm by using the molar extinction coefficient values provided by the manufacturer. $Cu(NO_3)_2{\cdot}3H_2O$ (>99.5%), NaCl (>99.5%), and KCl (>99.5%) were purchased from the Shanghai Chemical Reagent Company of the Chinese Medicine Group. 3-(*N*-morpholino)propanesulfonic acid (MOPS) was purchased from Sangon. Water purified on a Milli-Q A10 water purification system (specific resistance of 18.2 MΩ at 25 °C) was used for all experiments. Dienophiles **1a–c**, **4a–d** and their corresponding racemic products were synthesized according to the literature (see the Supporting Information for details).

Typical experimental procedure for catalytic Diels–Alder reaction; aza-chalcones as dienophile: An aqueous solution of G_4-DNA (G_4 unit, 50 μM final) was added to MOPS buffer (1 mL, 20 mM, pH 6.5) containing NaCl (50 mM) or KCl (150 mM). After this mixture had been stirred for 30 min at 4 °C, a solution of $Cu(NO_3)_2$ (10 μM final) was added. Then, aza-chalcone **1** in CH_3CN (10 μL of a 0.1 M solution) and freshly distilled cyclopentadiene **2** (15 μL)

were added. The mixture was stirred for 12 h (**1a**) or 72 h (**1b** and **1c**) at 4 °C, followed by extraction with diethyl ether, and drying over Na_2SO_4. The organic phase was removed under reduced pressure. The residue was directly analyzed by ^{1}H NMR and HPLC. The conversions were determined by ^{1}H NMR and HPLC (only for **3a**).

UV/Vis spectroscopy: UV-Vis experiments were carried out on a model 2450 spectrophotometer (Shimadzu, Japan) equipped with a Peltier temperature-control accessory. All spectra were measured with a sealed quartz cell (path length 1.0 cm).

Circular dichroism (CD) spectroscopy: All CD spectra were recorded on a dual-beam DSM 1000 CD spectrophotometer (Olis, Bogart, GA) with a 10 mm path-length quartz cell (220–320 nm, 4 °C, under N_2 purge, scan rate 0.5 nm s^{-1}). The background CD spectrum was subtracted from the average scan for each sample in the corresponding buffer solution. The molarities refer to the G-quadruplex unit. CD samples of all G-quadruplexes were prepared at a concentration (G_4 unit) of 5 μM in MOPS (20 mM, pH 6.5) with NaCl (50 mM) or KCl (150 mM).

^{1}H NMR spectroscopy: All ^{1}H NMR spectra were recorded at 400 MHz in $CDCl_3$, with TMS or residual protic solvent as the internal standard.

HPLC analysis: Enantioselectivity was determined with a model 1260 HPLC device (Agilent Technologyies) at 25 °C with a Chiralpak ODH, AD, ADH, or AD column (Daicel, Tokyo, Japan) and a UV detector (eluents: isopropanol and n-hexane).

Continuous wave (CW) X-band electron paramagnetic resonance (EPR) spectroscopy: Measurement was carried out on a Bruker A200 electron-spin resonance spectrometer (microwave frequency 9.3 GHz; power 5.0 mW; modulation amplitude 6G; modulation frequency 100 KHz). EPR spectra were recorded at 100 K in a frozen aqueous solution under nitrogen. Easyspin (http://www.easyspin.org/) was used for spectral simulation; parameters were determined for the frozen solution spectra by using the fitting function "pepper". EPR sample preparation: G_4-DNA-K samples were prepared by dissolving HT21, HT45, or HT69 in MOPS (20 mM) containing KCl (150 mM). Then aqueous $Cu(NO_3)_2$ was added to G_4-DNA-K buffer solution to obtain theh G_4-DNA-K-Cu complex; the concentration of Cu^{II} was 300 μM, and the ratio of G_4-DNA (in G_4 unit) to Cu^{II} was 2:1. glycerol (10%, *v/v*) was added to the buffer to aid "glassy state" formation.

Acknowledgements

We thank Prof. Yan Liu, Dr. Jun Zhou, Dr. Shengmei Lu and Dr. Jun Li for their helpful discussions, Prof. Jun Chen, Prof. Zong K. Zhao and Dr. Sufang Zhang for their help in experiments. We thank Dr. Wei Tong from High Magnetic Field Laboratory of Chinese Academy of Sciences for his help in EPR experiment and Guoguo Tan from Lanzhou University for his help in EPR analysis. This work is financially supported by National Natural Science Foundation of China (grant numbers 31000392, 21173213).

Keywords: Diels–Alder reaction · DNA · enantioselective catalysis · G-quadruplexes · human telomeric DNA · metalloenzyme

[1] a) G. Roelfes, *Mol. BioSyst.* **2007**, *3*, 126–135; b) A. Jäschke in *Molecular Encapsulation: Organic Reactions in Constrained Systems* (Eds.: U. H. Brinker, J.-L. Mieusset), Wiley, Hoboken, **2010**, pp. 377–396.

[2] a) B. Seelig, S. Keiper, F. Stuhlmann, A. Jäschke, *Angew. Chem. Int. Ed.* **2000**, *39*, 4576–4579; *Angew. Chem.* **2000**, *112*, 4764–4768; b) F. Stuhlmann, A. Jäschke, *J. Am. Chem. Soc.* **2002**, *124*, 3238–3244; c) A. Serganov, S. Keiper, L. Malinina, V. Tereshko, E. Skripkin, C. Höbartner, A. Polonskaia, A. T. Phan, R. Wombacher, R. Micura, Z. Dauter, A. Jäschke, D. J. Patel, *Nat. Struct. Mol. Biol.* **2005**, *12*, 218–224.

[3] a) A. J. Boersma, R. P. Megens, B. L. Feringa, G. Roelfes, *Chem. Soc. Rev.* **2010**, *39*, 2083–2092; b) S. Park, H. Sugiyama, *Angew. Chem. Int. Ed.* **2010**, *49*, 3870–3878; *Angew. Chem.* **2010**, *122*, 3960–3969; c) S. K. Silverman, *Angew. Chem. Int. Ed.* **2010**, *49*, 7180–7201; *Angew. Chem.* **2010**, *122*, 7336–7359; d) J. Bos, G. Roelfes, *Curr. Opin. Chem. Biol.* **2014**, *19*, 135–143.

[4] a) G. Roelfes, B. L. Feringa, *Angew. Chem. Int. Ed.* **2005**, *44*, 3230–3232; *Angew. Chem.* **2005**, *117*, 3294–3296; b) D. Coquière, B. L. Feringa, G. Roelfes, *Angew. Chem. Int. Ed.* **2007**, *46*, 9308–9311; *Angew. Chem.* **2007**, *119*, 9468–9471; c) N. S. Oltra, G. Roelfes, *Chem. Commun.* **2008**, 6039–6041; d) A. J. Boersma, B. L. Feringa, G. Roelfes, *Angew. Chem. Int. Ed.* **2009**, *48*, 3346–3348; *Angew. Chem.* **2009**, *121*, 3396–3398; e) A. J. Boersma, D. Coquière, D. Geerdink, F. Rosati, B. L. Feringa, G. Roelfes, *Nat. Chem.* **2010**, *2*, 991–995.

[5] J. Wang, E. Benedetti, L. Bethge, S. Vonhoff, S. Klussmann, J.-J. Vasseur, J. Cossy, M. Smietana, S. Arseniyadis, *Angew. Chem. Int. Ed.* **2013**, *52*, 11546–11549; *Angew. Chem.* **2013**, *125*, 11760–11763.

[6] a) A. Rich, *Gene* **1993**, *135*, 99–109; b) D. E. Gilbert, J. Feigon, *Curr. Opin. Struct. Biol.* **1999**, *9*, 305–314; c) J. Choi, T. Majima, *Chem. Soc. Rev.* **2011**, *40*, 5893–5909.

[7] a) J. R. Williamson, *Annu. Rev. Biophys. Biomol. Struct.* **1994**, *23*, 703–730; b) S. Neidle, G. N. Parkinson, *Curr. Opin. Struct. Biol.* **2003**, *13*, 275–283; c) M. Gellert, M. N. Lipsett, D. R. Davies, *Proc. Natl. Acad. Sci. USA* **1962**, *48*, 2013–2018.

[8] a) Y. Wang, D. J. Patel, *Structure* **1993**, *1*, 263–282; b) S. Burge, G. N. Parkinson, P. Hazel, A. K. Todd, S. Neidle, *Nucleic Acids Res.* **2006**, *34*, 5402–5415; c) D. J. Patel, A. T. Phan, V. Kuryavyi, *Nucleic Acids Res.* **2007**, *35*, 7429–7455; d) J. Kypr, I. Kejnovská, D. Renčiuk, M. Vorlíčková, *Nucleic Acids Res.* **2009**, *37*, 1713–1725; e) A. T. Phan, *FEBS J.* **2010**, *277*, 1107–1117.

[9] a) D. M. Gray, J.-D. Wen, C. W. Gray, R. Repges, C. Repges, G. Raabe, J. Fleischhauer, *Chirality* **2008**, *20*, 431–440; b) S. Masiero, R. Trotta, S. Pieraccini, S. De Tito, R. Perone, A. Randazzo, G. P. Spada, *Org. Biomol. Chem.* **2010**, *8*, 2683–2692; c) A. Randazzo, G. P. Spada, M. W. da Silva in *Quadruplex Nucleic Acids, Vol. 330* (Eds.: J. B. Chaires, D. Graves), Springer, Berlin, **2013**, pp. 67–86.

[10] a) S. Roe, D. J. Ritson, T. Garner, M. Searle, J. E. Moses, *Chem. Commun.* **2010**, *46*, 4309–4311; b) M. Wilking, U. Hennecke, *Org. Biomol. Chem.* **2013**, *11*, 6940–6945; c) C. Wang, G. Jia, J. Zhou, Y. Li, Y. Liu, S. Lu, C. Li, *Angew. Chem. Int. Ed.* **2012**, *51*, 9352–9355; *Angew. Chem.* **2012**, *124*, 9486–9489; d) C. Wang, Y. Li, G. Jia, Y. Liu, S. Lu, C. Li, *Chem. Commun.* **2012**, *48*, 6232–6234; e) C. Wang, G. Jia, Y. Li, S. Zhang, C. Li, *Chem. Commun.* **2013**, *49*, 11161–11163.

[11] a) W. E. Wright, V. M. Tesmer, K. E. Huffman, S. D. Levene, J. W. Shay, *Genes Dev.* **1997**, *11*, 2801–2809; b) H.-Q. Yu, D. Miyoshi, N. Sugimoto, *J. Am. Chem. Soc.* **2006**, *128*, 15461–15468; c) Y. Xu, T. Ishizuka, K. Kurabayashi, M. Komiyama, *Angew. Chem. Int. Ed.* **2009**, *48*, 7833–7836; *Angew. Chem.* **2009**, *121*, 7973–7976; d) L. Petraccone, C. Spink, J. O. Trent, N. C. Garbett, C. S. Mekmaysy, C. Giancola, J. B. Chaires, *J. Am. Chem. Soc.* **2011**, *133*, 20951–20961; e) H. Yu, X. Gu, S.-i. Nakano, D. Miyoshi, N. Sugimoto, *J. Am. Chem. Soc.* **2012**, *134*, 20060–20069.

[12] L. Stefan, F. Denat, D. Monchaud, *J. Am. Chem. Soc.* **2011**, *133*, 20405–20415.

[13] a) A. Cummaro, I. Fotticchia, M. Franceschin, C. Giancola, L. Petraccone, *Biochimie* **2011**, *93*, 1392–1400; b) C. Zhao, L. Wu, J. Ren, Y. Xu, X. Qu, *J. Am. Chem. Soc.* **2013**, *135*, 18786–18789; c) X.-X. Huang, L.-N. Zhu, B. Wu, Y.-F. Huo, N.-N. Duan, D.-M. Kong, *Nucleic Acids Res.* **2014**, *42*, 8719–8731.

[14] K.-i. Shinohara, Y. Sannohe, S. Kaieda, K.-i. Tanaka, H. Osuga, H. Tahara, Y. Xu, T. Kawase, T. Bando, H. Sugiyama, *J. Am. Chem. Soc.* **2010**, *132*, 3778–3782.

[15] a) K. N. Luu, A. T. Phan, V. Kuryavyi, L. Lacroix, D. J. Patel, *J. Am. Chem. Soc.* **2006**, *128*, 9963 – 9970; b) Y. Xu, Y. Noguchi, H. Sugiyama, *Bioorg. Med. Chem.* **2006**, *14*, 5584 – 5591; c) J. Dai, M. Carver, D. Yang, *Biochimie* **2008**, *90*, 1172 – 1183.

[16] a) S. Haider, G. N. Parkinson, S. Neidle, *Biophys. J.* **2008**, *95*, 296 – 311; b) L. Petraccone, J. O. Trent, J. B. Chaires, *J. Am. Chem. Soc.* **2008**, *130*, 16530 – 16532; c) L. Bauer, K. Tlučková, P. Tóthová, V. Viglaský, *Biochemistry* **2011**, *50*, 7484 – 7492; d) I. Fotticchia, C. Giancola, L. Petraccone, *Chem. Commun.* **2013**, *49*, 9488 – 9490.

[17] M. V. Clausen, H. Poulsen in *Metallomics and the Cell, Vol. 12* (Ed.: L. Banci), Springer, New York, **2013**, pp. 41 – 67.

[18] A. T. Phan, V. Kuryavyi, K. N. Luu, D. J. Patel, *Nucleic Acids Res.* **2007**, *35*, 6517 – 6525.

[19] a) J. Podtetenieff, A. Taglieber, E. Bill, E. J. Reijerse, M. T. Reetz, *Angew. Chem. Int. Ed.* **2010**, *49*, 5151 – 5155; *Angew. Chem.* **2010**, *122*, 5277 – 5281; b) E. I. Solomon, D. E. Heppner, E. M. Johnston, J. W. Ginsbach, J. Cirera, M. Qayyum, M. T. Kieber-Emmons, C. H. Kjaergaard, R. G. Hadt, L. Tian, *Chem. Rev.* **2014**, *114*, 3659 – 3853.

Received: December 8, 2014
Published online on February 11, 2015

